Catalysis Today 150 (2010) 186–195

Contents lists available at ScienceDirect

Catalysis Today

journal homepage: www.elsevier.com/locate/cattod

Factors controlling the development of the HYD route of desulfurization of DBT over γ-alumina supported Pt and Pd catalysts

V.G. Baldovino-Medrano [a], P. Eloy [b], E.M. Gaigneaux [b], S.A. Giraldo [a], Aristóbulo Centeno [a,*]

[a] Centro de Investigaciones en Catálisis (CICAT), Escuela de Ingeniería Química, Universidad Industrial de Santander (UIS), Cra. 27 Calle 9, Bucaramanga, Santander, Colombia
[b] Université catholique de Louvain, Unité de catalyse et chimie des matériaux divisés, Croix du Sud 2/17, B-1348 Louvain-la-Neuve, Belgium

ARTICLE INFO

Article history:
Available online 9 September 2009

Keywords:
$Pt/\gamma\text{-}Al_2O_3$
$Pd/\gamma\text{-}Al_2O_3$
Chlorides
Pretreatment conditions
Dibenzothiophene
HYD pathway
Acidity

ABSTRACT

The influence of the metallic precursor and the pretreatment of γ-alumina supported Pt and Pd catalysts on the reactivity of dibenzothiophene (DBT) over these materials was studied. It was found that the use of chlorided precursors induces changes in the chemical state of the metals and in the acidic properties of the supported catalysts which are partly a function of the type of noble metal. Such changes were found to positively affect the conversion of DBT over both monometallic systems. Regardless of the preparation conditions, Pt possesses a high activity and a high selectivity to the direct route of desulfurization of DBT, whereas Pd is less active but performs HDS with a strong tendency to develop the hydrogenation route of desulfurization (HYD) when employing a chlorided precursor. The use of a low temperature pretreatment of the chlorided catalysts enhanced DBT conversion, and for $Pd/\gamma\text{-}Al_2O_3$ it doubled the selectivity to HYD. The registered trends were considered to be rather related to a change in the distribution of acidic sites of the catalysts and to changes in the chemical state of the noble metals than to the effect of dispersion.

1. Introduction

Either alloyed or as monometallic catalysts Pt and Pd have shown very good catalytic performance in the hydrodesulfurization (HDS) of dibenzothiophene (DBT) type molecules [1–6]. 4,6-DimethylDBT is the most representative member of the family of highly refractory 4,6-alkyl-substituted DBTs, and is usually regarded as the target molecule to be hydropurified in heavy oil cuts [7,8]. Though the HDS of this molecule can proceed by the hydrogenation (HYD) or direct (DDS) routes of desulfurization, it has been both experimentally and theoretically demonstrated that the steric hindrance imposed by the alkyl-substituents of 4,6-dimethylDBT practically leaves no room for the scission of the sulfur heteroatom via DDS [7–9]; thus making conversion via HYD essential to achieve the required rate of HDS [7,8]. Within this frame, it is very desirable to develop catalytic systems able to selectively develop the HYD route of hydrodesulfurization. Keeping this objective in mind, the use of DBT as a model molecule is more convenient, in respect to 4,6-dimethylDBT, to test the intrinsic selectivity of a given catalyst to HYD over DDS. A material highly selective to HYD during the HDS of dibenzothiophene will clearly present a higher rate of HDS when tested with 4,6-dimethylDBT, as it can be evidenced in a recent report by Wang et al. [10]. To accomplish this goal, it is quite important to understand those factors which control the development of HYD. Several studies indicate that the particular nature of the noble metals, Pd or Pt, and the chemical properties of the support are crucial for HYD [1–6,10]. Moreover, the reactivity of DBT over Pt and Pd is remarkably different [1,3–6,11–13]. Comparing the reported behavior for supported Pt and Pd catalysts in this reaction, one can easily realize that Pt is highly active and selective to DDS, whereas Pd has a lower activity but HYD can be more competitive to DDS [3–5,11–13]. On the other hand, an increase in the acidity of the support can enhance HYD reaction rates [10,14–16]. Acidic supports can also improve the resistance of the noble metals to sulfidation increasing their activity in aromatics hydrogenation under HDS environments [17–21]. $\gamma\text{-}Al_2O_3$ supported Pt and Pd catalysts are known as bifunctional catalysts [20,22,23]. Their chemical characteristics can be modified in many possible ways, ranging from the selection of the metallic precursor [1,24–34] to the conditions used in the activation stage [1,5,6,11,35–37].

In this study, it was decided to study the specific influence of the use of two different metallic precursors, organometallic and chlorided Pt and Pd precursors, and the conditions used during the pretreatment of the catalysts; before performing the HDS of dibenzothiophene, in the selectivity to HYD. Catalysts were characterized by H_2 and NH_3 chemisorption, temperature programmed reduction (TPR) and X-ray photoelectron spectroscopy (XPS).

* Corresponding author. Tel.: +57 7 6344746; fax: +57 7 6344684.
E-mail addresses: acenteno@uis.edu.co, aristo.cen.47@gmail.com (A. Centeno).

0920-5861/$ – see front matter © 2009 Elsevier B.V. All rights reserved.
doi:10.1016/j.cattod.2009.07.106

2. Experimental

2.1. Catalysts preparation

A series of γ-alumina (Procatalyse, S_{BET} = 220 m^2/g, Vp = 0.62 cm^3/g, Dp = 11.6 nm) supported Pt and Pd catalysts were prepared by three different methods. The first method consisted in the impregnation of the support with Pd(II) acetylacetonate ($Pd(acac)_2$) and Pt(II) acetylacetonate ($Pt(acac)_2$) (Sigma–Aldrich) precursors, diluted in toluene, followed by drying (12 h, T = 393 K) and calcination in air flow (4 h, T = 773 K). The second one consisted in the impregnation of the support with chlorided precursors: aqueous solutions of $PdCl_2$ and H_2PtCl_6 (Sigma–Aldrich), followed by drying and calcination under the same conditions of the first method. Catalysts prepared with these two methods were in situ reduced before the catalytic tests at 673 K for 3 h. And finally, the third method consisted in treating the same catalysts prepared by method 2 by drying at 363 K for 6 h and reduction at 473 K for 4 h. Catalysts were labeled according to each preparation method as follows: Pt(MC),Pd(MC)-Org for the first method; Pt(MC),Pd(MC)-Cl-HT for the second one (HT = high temperature), and Pt(MC),Pd(MC)-Cl-LT for the third one (LT = low temperature). MC stands for the metallic content of the catalysts as obtained from atomic absorption.

2.2. Catalyst characterization

2.2.1. Hydrogen chemisorption

H_2 chemisorption measurements were performed in a Micromeritics ASAP 2010C instrument. The pretreatment of the samples (ca. 0.15 g) comprised an initial evacuation stage under He flow for 30 min at the temperature selected for the measurement, followed by oxidation under O_2 flow; reproducing the conditions of catalyst's calcination described in Section 2.1. Subsequent evacuations under He flow were carried out, each one for 30 min, at the employed oxidation temperature and at the temperature selected for the measurements. Afterward, in situ reduction in hydrogen at the corresponding conditions of the catalytic test was performed, i.e. samples of Pt(MC),Pd(MC)-Org and Pt(MC),Pd(MC)-Cl-HT catalysts were reduced at 673 K, and the samples of Pt(MC),Pd(MC)-Cl-LT were reduced at 473 K. After this step, evacuation was performed by flowing He for 2 h at the employed reduction temperature under vacuum for 30 min, and finally under vacuum at the temperature selected for the measurement for another 30 min. H_2 chemisorption isotherms were determined at 308 K for Pt catalysts and at 343 K for Pd ones; thus, avoiding the formation of the β-Pd-H hydride phase [38], this was also verified by TPR measurements. The reported H_2 uptake values were taken from the volume difference between two H_2 adsorption isotherms; the second one measured after an evacuation time of 45 min, extrapolated to zero pressure (strongly adsorbed hydrogen).

2.2.2. Ammonia chemisorption

NH_3 chemisorption measurements were carried out at 308, 423 and 623 K in a Micromeritics ASAP 2010C apparatus. Samples of the catalysts were pretreated following the same protocol employed during H_2 chemisorption measurements (Section 2.2.1). By using this protocol, the obtained results describe the acidity of the catalysts at the beginning of the catalytic tests. Acidic sites' strength was classified as: weak (measured at 308 K), medium (measured at 423 K) and strong (measured at 623 K), as in agreement with a previous work [39]. The total number of acidic sites was defined as the algebraic sum weak + medium + strong acidic sites. According to the strength of the acid sites, the ratio: (number of corresponding acidic site)/(total number of acidic sites) was defined. The method for the evaluation of the amount of NH_3 chemisorbed was similar to that used in H_2 chemisorption.

2.2.3. Temperature programmed reduction (TPR)

TPR experiments were performed in a u-shaped fixed-bed quartz micro-reactor containing samples of ca. 0.1 g of the different prepared catalysts to which a layer of approximately 1 cm of glass beads was added as to guaranty plug-flow. Before the analysis, drying of the samples under He flow was performed at 413 K until stabilization of the H_2O signal as registered with a QMC 311 Balzers quadrupole mass spectrometer coupled to the reactor. After cooling the reactor, TPR patterns were then registered by increasing temperature from 308 to 1073 K at a temperature rate of 10 K/min. TPR analysis was performed by flowing a 5 vol.% H_2 in He (flow rate = 50 mL/min) gas mixture. The MS signals corresponding to H_2 (m/e = 2), H_2O (m/e = 18), HCl (m/e = 36) and Cl^+ (m/e = 37); corresponding to diverse chlorine containing compounds, were monitored. Recorded signals were treated by using a Gaussian mathematical function.

2.2.4. X-ray photoelectron spectroscopy (XPS)

XPS analyses were performed on samples of the catalysts either in the oxidized (calcined: -Org and HT- or dried -LT catalysts-) or activated states with a Kratos Axis Ultra spectrometer (Kratos Analytical, Manchester, UK) equipped with a monochromatised Al X-ray source (powered at 10 mA and 15 kV). The sample powders were pressed into small stainless steel troughs mounted on a multi-specimen holder. The pressure in the analysis chamber was around 10^{-6} Pa. The angle between the normal to the sample surface and the lens axis was 0°. The hybrid lens magnification mode was used with the slot aperture resulting in an analyzed area of 700 μm × 300 μm. The pass energy was set at 40 eV. In these conditions, the energy resolution gives a full width at half maximum (FWHM) of the Ag $3d_{5/2}$ peak of about 1.0 eV. Charge stabilization was achieved by using the Kratos Axis device. The following sequence of spectra was recorded: survey spectrum, C 1s, O 1s, Al 2p, Al 2s, Pd 3d, Pt 4d, Cl 2p, and C 1s again to check the stability of charge compensation in function of time and the absence of degradation of the sample during the analyses. The binding energies (BE) were calculated with respect to the C–(C,H) component of the C 1s peak fixed at 284.8 eV. The spectra were decomposed with the CasaXPS program (Casa Software Ltd., UK) with a Gaussian/Lorentzian (70/30) product function after subtraction of a linear baseline. Molar fractions were calculated using peak areas normalized on the basis of acquisition parameters, sensitivity factors provided by the manufacturer and the transmission function. The Pd 3d doublet was decomposed in three components with Pd $3d_{5/2}$ binding energies fixed at 335 (Pd^0), 336 (Pd^{2+}) and 338 eV (Pd^{4+}) [25]. To perform such decomposition the FWHM value of every component was mathematically fixed to comply with the criterion FWHM < 2.6. The algebraic sum of the surface atomic concentration of (Pd^{2+} + Pd^{4+}) species was defined as the total concentration of surface electron deficient $Pd^{\delta+}$ species. For the Pt 4d peak the energy separation for the doublet was fixed at 16.8 eV [24].

2.3. Catalytic tests

Catalysts were in situ activated before catalytic tests. Samples of 0.5 g of the calcined catalysts were dried at 393 K under N_2 flow for 1 h and subsequently, they were reduced in hydrogen flow (100 mL/min) at the conditions described in Section 2.1. Catalysts were tested in the HDS of dibenzothiophene (Sigma–Aldrich, 98%) using a continuous-flow high-pressure fixed-bed reactor. The composition of the liquid charge was 2 wt.% DBT and 2 wt.% hexadecane (Sigma–Aldrich, 98%); as chromatography internal

Table 1
H_2 and NH_3 chemisorption results for the prepared γ-Al_2O_3 supported Pd and Pt catalysts.

Catalyst[a]	n_{ads}^{STP} (μmol H_2/μmol metal)	n_{ads}^{STP} (μmol NH_3/g cat.)			
		T (K)			Total number of sites
		308	423	623	
γ-Al_2O_3	–	376.0	236.5	65.7	678.1
Pd(1.8)-Org	0.13	390.4	197.1	88.6	676.1
Pd(1.4)-Cl-LT	0.10	481.9	168.4	135.1	785.4
Pd(1.4)-Cl-HT	0.21	601.1	393.9	105.0	1101.0
Pt(1.4)-Org	0.29	361.4	218.2	69.6	649.3
Pt(1.1)-Cl-LT	0.38	443.0	190.9	105.8	739.7
Pt(1.1)-Cl-HT	0.56	527.1	289.9	178.0	995.0

[a] Pt(MC),Pd(MC)-Org = catalysts prepared from acetylacetonate precursors, calcined at 773 K and activated by H_2 reduction at 673 K; Pt(MC),Pd(MC)-Cl-LT = catalysts prepared from chlorided precursors, dried at 363 K and activated by H_2 reduction at 473 K; Pt(MC),Pd(MC)-Cl-HT = catalysts prepared from chlorided precursors and treated as those prepared with organometallic precursors. MC = metallic content as determined by atomic absorption. STP = standard temperature and pressure.

standard, dissolved in cyclohexane (commercial grade) with a total feed flow of 30 mL/h. Reaction conditions were those typical of HDS processes: T = 583 K, P = 5 MPa, and H_2/liquid feed ratio of 500 NL/L. The absence of any diffusion limitations was previously verified.

Liquid products were analyzed using a HP 6890 GC equipped with an FID, an HP-1 capillary column (100 m × 0.25 mm × 0.5 μm) and a split injector. Catalytic tests were conducted until reaching the steady state. Reaction products detected were: biphenyl (BP), cyclohexylbenzene (CHB) and hydrogenated intermediates: tetrahydro-dibenzothiophene (THDBT) and hexahydro-dibenzothiophene (HHDBT).

Activity was expressed as the conversion of DBT ($\%C_{DBT}$), products distribution as the yield ($\%y$) to each reaction product. $\%y$ was defined as the concentration of each reaction product detected in the GC analysis of collected liquid samples per total concentration of detected reaction products including DBT. Selectivity to HYD (S_{HYD}) was defined as the $(\%C_{DBT} - \%y_{BP})/\%y_{BP}$ ratio.

3. Results and discussion

3.1. Chemical properties of the prepared catalysts

The results of H_2 and NH_3 chemisorption are displayed in Table 1. H_2 uptake, expressed as μmol H_2/μmol metal, followed the order: Pd(1.4)-Cl-HT > Pd(1.8)-Org > Pd(1.4)-Cl-LT, for Pd, and Pt(1.1)-Cl-HT > Pt(1.1)-Cl-LT > Pt(1.4)-Org, for Pt. For the chlorided Pd and Pt catalysts, the high temperature treatment increased H_2 uptake capacity compared to the low temperature treatment. Dispersion values of the noble metals as obtained from these measurements are not presented here due to fact that overestimation resulting from the hydrogen spillover phenomena for γ-Al_2O_3 supported Pt and Pd

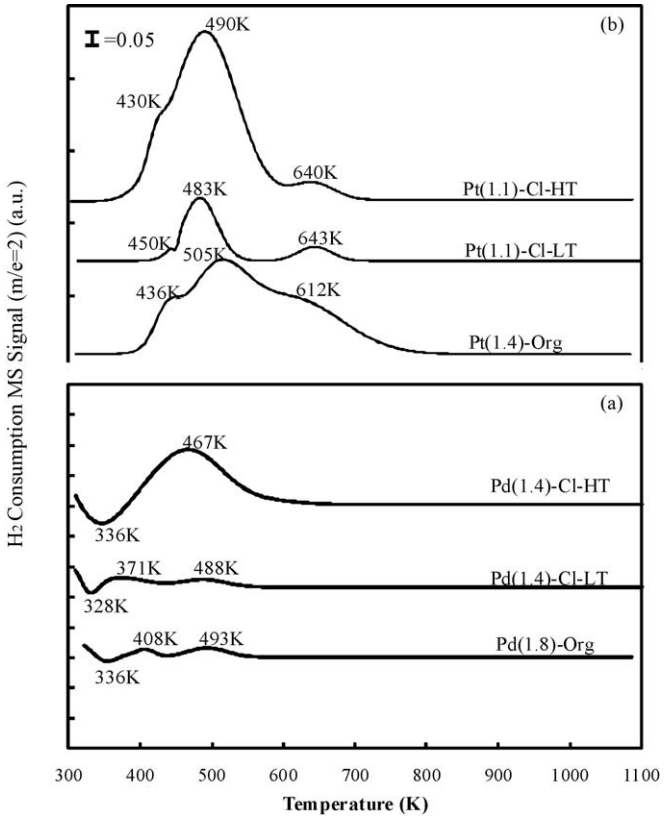

Fig. 1. TPR patterns for the prepared Pd and Pt catalysts: (a) Pd catalysts; (b) Pt catalysts. The H_2 Mass Spectrometer Signals are inverted.

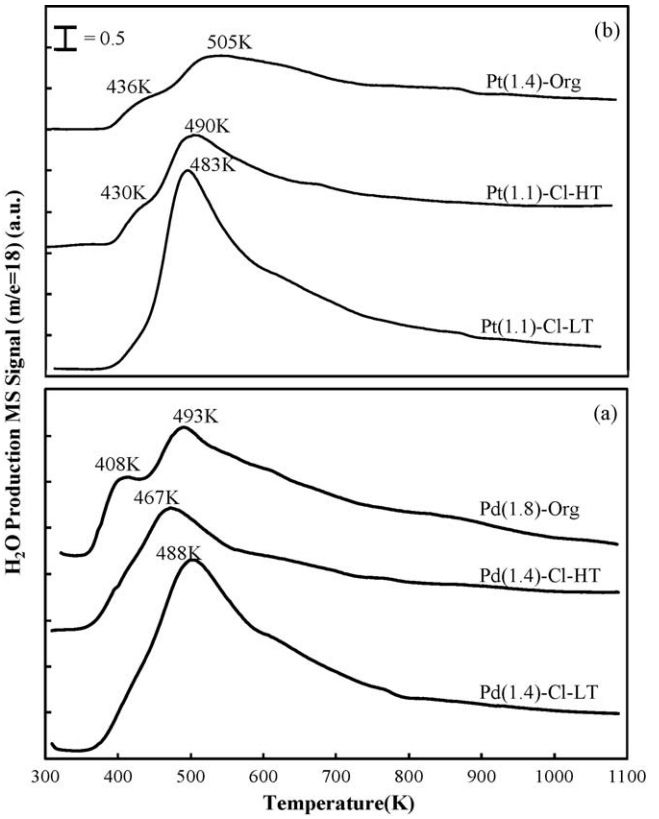

Fig. 2. H_2O production MS signal (m/e = 18) registered during the TPR analysis of the prepared Pd and Pt catalysts: (a) Pd catalysts; (b) Pt catalysts.

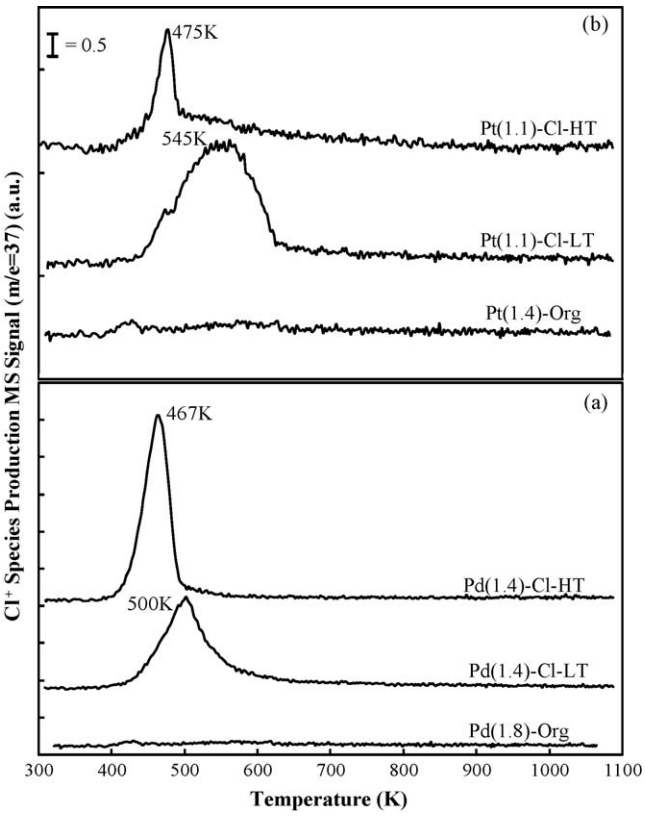

Fig. 3. Cl^+ species production MS signal (m/e = 37) registered during the TPR analysis of the prepared Pd and Pt catalysts: (a) Pd catalysts; (b) Pt catalysts.

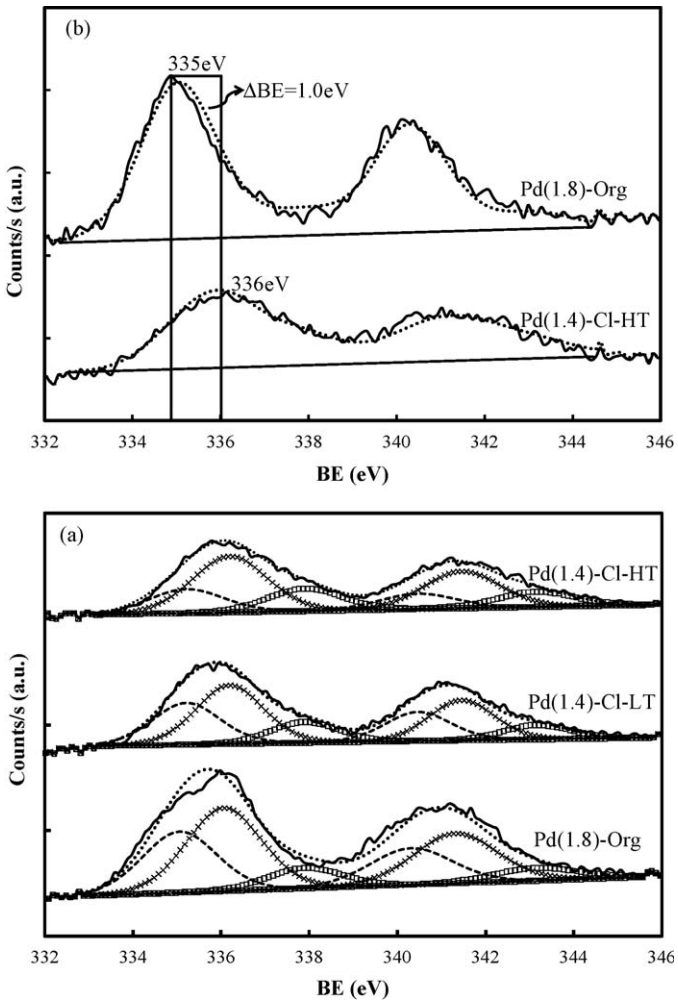

Fig. 4. XPS spectra of Pd/γ-Al_2O_3 catalysts before (a) and after activation (b). (- - -) Pd $3d_{5/2}$ at 335 eV (Pd^0); (×××) Pd $3d_{5/2}$ at 336 eV (Pd^{2+}) and (□□□) Pd $3d_{5/2}$ at 338 eV (Pd^{4+}).

cannot be completely ruled out [18,19,40]. Pd catalysts were found to possess a lower H_2 uptake capacity than Pt ones. This fact cannot be attributed to the formation of β-Pd-H hydrides. Fig. 1 shows the TPR patterns of the γ-Al_2O_3 supported Pd and Pt catalysts and Figs. 2 and 3 the MS signals corresponding to H_2O (m/e = 18) and to Cl^+ species (m/e = 37) obtained during such experiments. Though the signal attributed to HCl was also monitored in this case, it is not presented here because it basically can be overlapped with that of Cl^+. It can be seen in Fig. 1a that the peak corresponding to β-Pd-H appears below 343 K [38]; which is the temperature selected for the H_2 chemisorption experiments for Pd. Therefore, it can be assumed that, in general, regardless of the preparation method, the Pd catalysts have an intrinsically lower capacity to chemisorb hydrogen than Pt ones. Finally, as observed in Table 1, calcination at 773 K significantly enhanced the H_2 uptake capacity of the catalysts.

The oxidation state of the calcined catalysts was studied by XPS and the results are presented in Table 2 and Fig. 4 for Pd, and in Table 3 and Fig. 5 for Pt. As described in Section 2.2.4, the Pd 3d doublet was decomposed into three components; Pd^0, Pd^{2+} and Pd^{4+}, the ratio $Pd^{\delta+}/Pd^0$ being estimated. The presence of zero valent metallic particles in the calcined samples can be partly attributed to reduction of the noble metal in the analysis chamber of the instrument [24]. It can be observed in Table 2 that the ratio $Pd^{\delta+}/Pd^0$ is highest for Pd(1.4)-Cl-HT, whereas Pd(1.8)-Org and Pd(1.4)-Cl-LT display closer values, with the latter exhibiting a slightly higher ratio. Surface chlorine after calcination was detected for the samples of Pd/γ-Al_2O_3 prepared from $PdCl_2$, as in agreement with many literature reports [24–29,32]. This was also evidenced by the detection of MS peaks attributed to chlorine containing species during the TPR analysis (Fig. 3). In general, residual chlorine remains in the surface of the chlorided noble metal catalysts even after activation by reduction (Tables 2 and 3). Several literature reports agree with this result

Table 2
XPS analysis of the prepared Pd/γ-Al_2O_3 catalysts before and after activation.

Catalyst	State	335 eV (Pd^0)	336 eV (Pd^{2+})	338 eV (Pd^{4+})	Cl 2p		Al 2p		Atomic ratios		
		%At.	%At.	%At.	BE (eV)	%At.	BE (eV)	%At.	Pd/Al	$Pd^{\delta+}/Pd^0$	Cl/Al
Pd(1.8)-Org	Calcined	0.09	0.13	0.03	–	–	74.3	35.66	0.007	1.70	–
	Activated	0.15	0.02	0.02	–	–	74.4	31.51	0.006	0.25	–
Pd(1.4)-Cl-LT	Dried	0.10	0.14	0.05	198.3	0.99	74.3	35.55	0.008	1.92	0.028
	Activated	N.D.	N.D.	N.D.	N.D.	N.D.	N.D.	N.D.	N.D.	N.D.	N.D.
Pd(1.4)-Cl-HT	Calcined	0.04	0.13	0.05	198.3	0.56	74.3	36.25	0.006	4.02	0.016
	Activated	0.08	0.09	0.06	198.6	0.57	74.2	28.49	0.008	1.92	0.020

Table 3
XPS analysis of the prepared Pt/γ-Al_2O_3 catalysts before and after activation.

Catalyst	State	Pt 4d		Cl 2p		Al 2s		Atomic ratios	
		BE (eV)	%At.	BE (eV)	%At.	BE (eV)	%At.	Pt/Al	Cl/Al
Pt(1.4)-Org	Calcined	314.6	1.16	–	–	119.2	26.54	0.044	–
	Activated	314.7	1.60	–	–	119.4	24.53	0.065	–
Pt(1.1)-Cl-LT	Dried	315.9	0.33	198.3	0.83	119.3	25.02	0.013	0.033
	Activated	314.6	0.21	198.7	0.59	119.2	18.11	0.011	0.033
Pt(1.1)-Cl-HT	Calcined	315.5	0.29	198.4	0.62	119.2	24.76	0.012	0.025
	Activated	314.8	0.25	198.9	0.61	119.1	21.00	0.012	0.029

[24,26,28,29,34,41,42]. The above results picture a catalytic surface for calcined Pd/γ-Al_2O_3 composed of a mixture of metallic Pd^0, PdO, PdO_2 and/or $PdCl_xO_y$ species as in correspondence with the propositions of other authors [24,26,29,32,41]; the latter in the case of the use of the chlorided precursor. A change in the relative distribution of these different species can occur after reduction. This was evidenced by the changes in the $Pd^{\delta+}/Pd^0$ ratio after reduction presented in Table 2. Such change is of course due to the reduction of a part of the noble metal particles to the zero valent oxidation state. The fact that even some surface Pd^{4+} species remain after reduction in H_2 can be attributed to a strong metal–support interaction [17,20,24,42,43]. The process of adsorption of Pd and Pt acetylacetonate and chlorided precursors on γ-Al_2O_3 has been studied [30,44]. The extensive study conducted by Rob van Veen et al. [30] concluded that the acetylacetonate complexes of Pd and Pt chemisorb on the Al^{3+} CUS sites of γ-Al_2O_3 and physisorb on the γ-Al_2O_3 surface. These authors also established that the extent of Pt(acac)$_2$ adsorption on γ-Al_2O_3 is lower than that of Pd(acac)$_2$. In the case of the chlorided Pd and Pt precursors, the formation of chloro- and chloro(aquo)-palladate and platinate complexes in the presence of H^+ leads to surface charging of the –OH groups of alumina and further attachment of these complexes on the positively charged $–AlOH_2^+$ surface groups [31,45]. After pretreatment of the catalysts, either calcination or reduction, chlorine atoms are no longer attached to the metals, but remain in the vicinity of the Pt and Pd particles [42,46]. Fig. 1a displays the TPR patterns of the Pd catalysts. A peak corresponding to the decomposition of β-Pd-H hydride phase [38] was detected in all of the catalysts. Such peak was located at 336 K for both, Pd(1.8)-Org and Pd(1.4)-Cl-HT, catalysts which were calcined at the same temperature, and at 328 K for the Pd(1.4)-Cl-LT catalyst, which was only dried at 363 K. Both Pd(1.8)-Org and Pd(1.4)-Cl-LT exhibited two small reduction peaks instead of the wide reduction peak centered around 467 K displayed by Pd(1.4)-Cl-HT. These two peaks were found to be located at 408 and 493 K for Pd(1.8)-Org, and at 371 and 488 K for Pd(1.4)-Cl-LT, respectively. The TPR patterns displayed in Fig. 1b for Pt showed a wide peak of reduction for Pt(1.4)-Org with shoulders located at 436 and 612 K, respectively, and a maximum at 505 K. For the Pt(1.1)-Cl-HT, which has been prepared at the same calcination temperature, this peak was sharper and stronger with the maximum shifted to 490 K and the shoulders to 430 and 640 K, respectively. The Pt(1.1)-Cl-LT sample of the chlorided catalyst exhibited a very small shoulder a 450 K followed by the most intense peak at 483 K and a separated peak at 643 K. These peaks were attributed to a mixture of Pt species; PtO, PtO_2 and/or $PtCl_xO_y$ [26,29], which are analogous to those determined for Pd in XPS. The H_2O production MS signals presented in Fig. 2 are in good agreement with the TPR patterns of the catalysts. The shapes of these curves were very similar, but the H_2O signals were much more intense. Fig. 4 shows the XPS spectra of the oxidized and activated Pd catalysts. Fig. 4b clearly shows a BE shift ($\Delta BE \approx 1eV$) for the Pd 3d doublet of the Pd(1.4)-Cl-HT catalyst compared to Pd(1.8)-Org in the activated samples. The XPS results for Pt (Table 3) showed that the oxidation state of Pt in the chlorided catalysts, Pt(1.1)-Cl-HT and Pt(1.1)-Cl-LT, is alike, whereas the Pt 4d doublet for Pt(1.4)-Org was shifted to a lower BE, $\Delta BE \approx 1$ eV. This is indicative of the presence of Pt particles in an oxidation state closer to metallic Pt^0. The Pt 4d doublet presented in Fig. 5a illustrates the BE shift. Furthermore, a survey of the Pt 4f peak of these catalysts (Fig. 5b) shows, that contrary to the chlorided catalysts; for which the Pt 4f doublet is fully overlapped with the Al 2p line, the Pt 4f doublet of Pt(1.4)-Org is partially separated from Al 2p, at a BE of 71.0 eV. This is actually the position of metallic Pt^0. At this point it seems that this behavior does not match with the registered TPR pattern of this catalyst, because compared to the chlorided Pt samples it is observed that Pt(1.4)-Org is reduced at a higher temperature (Fig. 1a). However,

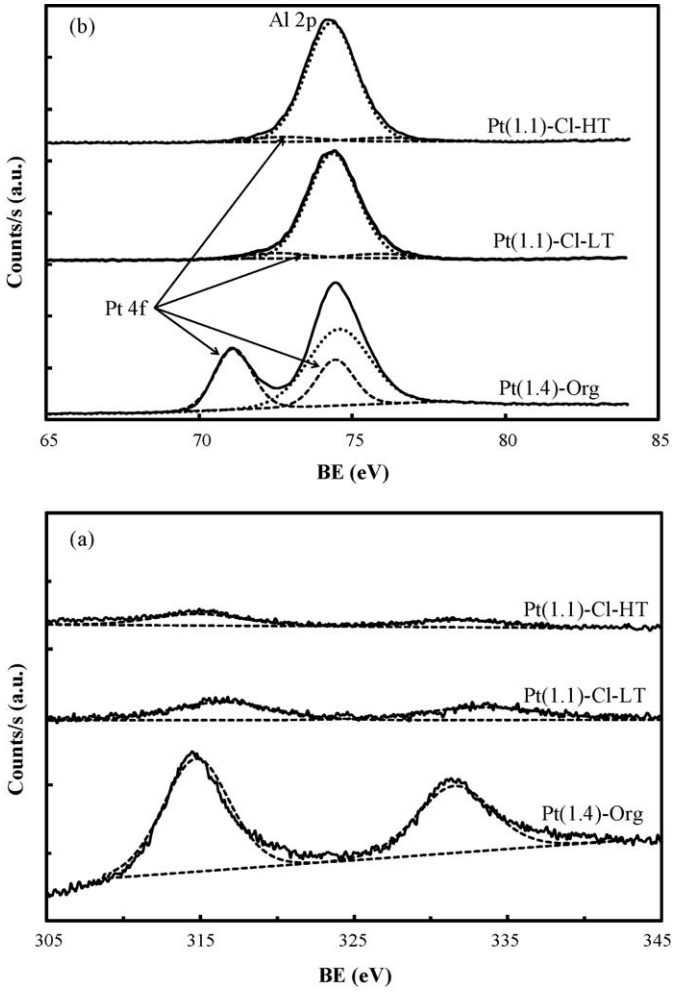

Fig. 5. XPS spectra of the Pt 4d doublet (a) and Al 2p line (b) of the Pt/γ-Al_2O_3 catalysts before activation.

various studies [28,33] have demonstrated that the Pt 4f doublet can be separated from Al 2p in those Pt/γ-Al_2O_3 catalysts containing high metallic contents in which sintered Pt particles are present. Another factor that could be playing a role in such trend is the possible formation of a spinel $PtAl_2O_4$ phase after calcination, which has a higher reduction temperature [26]. This is more plausible when using the $Pt(acac)_2$ precursor due to attachment of the to the Al^{3+} CUS sites of γ-Al_2O_3 [30] and not to –OH surface groups as in the case of the chlorided precursor [31,45]. The registered trend indicates that, as in the case of Pt, the Pd species present on those catalysts prepared from chlorides are more reducible than those obtained after preparation with the $Pd(acac)_2$ precursor. As in the case of Pt, the attachment of the $Pd(acac)_2$ complex to the Al^{3+} CUS sites of γ-Al_2O_3 instead to the –OH surface groups of the carrier could lead to the formation of Pd–Al species, such as $PdAl_2O_4$ which are reduced at higher temperatures [26]. For the samples of the catalyst prepared from the chlorided precursor, the wide peak centered at 467 K for the Pd(1.4)-Cl-HT sample reflects a complex pattern of reduction of the diverse Pd species of the catalyst. The TPR pattern of the dried sample (Pd(1.4)-Cl-LT) can be interpreted as the separation of two contributions of the wide peak of Pd(1.4)-Cl-HT. The existence of different Pd–Cl–alumina complexes after impregnation of aqueous $PdCl_2^{4-}$ in which Pd is surrounded and in direct contact with chlorine has been determined [45]. After calcination at 773 K, several studies demonstrate that these species are converted mostly to PdO, and partly to Pd^{4+}, with chlorine still attached to the Al_2O_3 support, but no longer directly linked to Pd [47,48]. The maximum located around 467 K in the TPR analysis of chlorided Pd/γ-Al_2O_3 catalysts is attributed to the reduction of the $PdCl_xO_y$ complex [48]. After calcination at 773 K there is a significant increase in the amount of $Pd^{\delta+}$ as compared to the concentration of Pd^0 rather due to a decrease in the surface concentration of Pd^0 than to a drastic change in the distribution of (Pd^{4+} + Pd^{2+}). The presence of the above described mixture of electron deficient and metallic noble metal particles remains after activation of the catalysts, with changes in the relative amount of each one of them due to the reduction with H_2 during the activation.

Concerning the acidic properties of the materials before the catalytic tests, the results of ammonia chemisorption are displayed in Table 1, and the (number of specific acid site)/(total number of acid sites) ratio (see Section 2.2.2 for details), is presented in Fig. 6. It can be seen in Table 1 that compared to the bare γ-Al_2O_3 support which was reduced at the same condition of the HT catalysts, the Pt and Pd catalysts prepared from acetylacetonates have a lower amount of total acidic sites. The Pd and Pt catalysts prepared from chlorides showed a higher amount of total acidic sites regardless of the pretreatment used. Pd catalysts had, in all cases, a higher concentration of acidic sites as compared to Pt ones, regardless the preparation conditions. It is interesting to follow the distribution of acidic sites according to their strength (Fig. 6). The distribution of weak, medium and strong acidic sites of those catalysts prepared from acetylacetonates was rather similar to that of the γ-Al_2O_3 support, indicating that the acidic properties of both materials are almost the same. Making a comparison of the referred acidity ratio between the Pd and Pt catalysts as a function of the preparation method the following behavior was observed: (i) those catalysts prepared with chlorides and by the LT treatment showed the highest relative amount of weak acidic sites, both for Pt and Pd, whereas those prepared with chlorides by the HT treatment exhibited the lowest relative amount of them. (ii) In the case of the Pd catalysts, the relative amount of medium acidic sites is registered for the Pd(1.4)-Cl-HT catalyst followed by Pd(1.8)-Org > Pd(1.4)-Cl-LT. This trend was not the same found for Pt, in this case: Pt(1.4)-Org > Pt(1.1)-Cl-HT > Pt(1.1)-Cl-LT. Finally, regarding the relative amount of strong acidic sites (iii), for Pd,

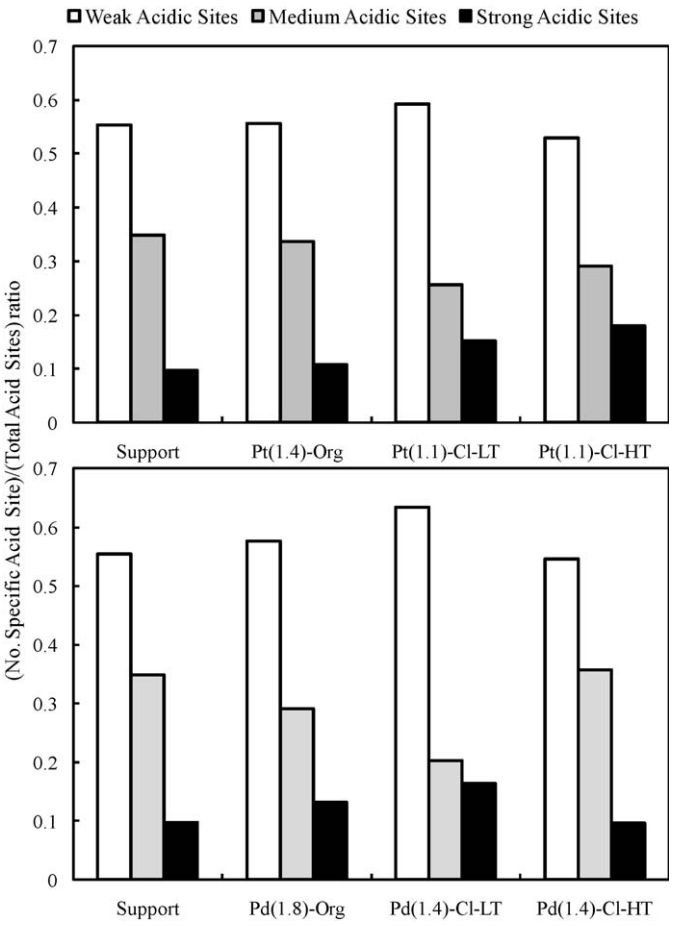

Fig. 6. Acidic sites distribution – (number of specific acid site)/(total number of acid sites) ratio – for the prepared Pd and Pt/γ-Al_2O_3 catalysts according to their strength. Number of weak acidic sites from NH_3 chemisorption at T = 308 K; number of medium acidic sites from NH_3 chemisorption at T = 423 K, and number of strong acidic sites from NH_3 chemisorption at T = 623 K.

it followed the order: Pd(1.4)-Cl-LT > Pd(1.8)-Org > Pd(1.4)-Cl-HT, and for Pt: Pt(1.1)-Cl-HT > Pt(1.1)-Cl-LT > Pt(1.4)-Org. The results described above evidence small differences in the acidic balance of the catalysts as a function of the noble metal. Furthermore, from the results for the chlorided catalysts and those of the ones prepared from acetylacetonates, it is clear that the presence of residual chlorine influences such acidic balance. It is well known that chlorine significantly modifies the acidic properties of γ-Al_2O_3 due to a polarization of its surface –OH groups [49,50]. During the decomposition of the metallic precursors, either in the calcination or activation stage, the interaction of the gaseous HCl produced has been found to induce the formation of new acidic sites on the alumina surface [49–51]. In particular, it seems that regardless of the calcination temperature of the catalyst, the formation of Brønsted acidic sites occurs when reduction at low temperatures takes place whereas at higher temperatures the apparition of strong Lewis acidic sites takes place [49–51]. The results of NH_3 chemisorption presented here are not useful to distinguish the precise nature of the acidic sites induced by chlorine but reflect that indeed changes in the distribution of the strength of the acidic sites of the catalysts are happening during the pretreatment stage.

3.2. Catalytic performance in the HDS of dibenzothiophene

The conversion of DBT and the yield to the different reaction products: BP, CHB, THDBT and HHDBT, as a function of the preparation method are presented in Fig. 7 for Pd and in Fig. 8 for

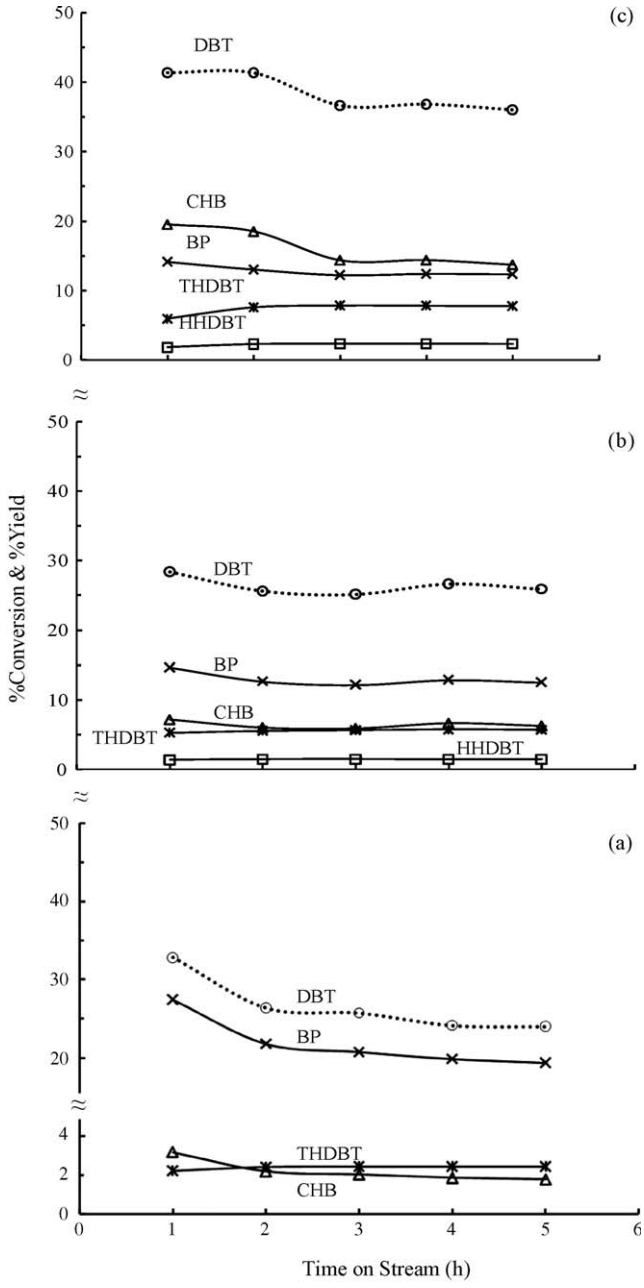

Fig. 7. Evolution with time on stream of the conversion of dibenzothiophene over the prepared Pd/γ-Al_2O_3 catalysts: (a) Pd(1.8)-Org; (b) Pd(1.4)-Cl-HT; (c) Pd(1.4)-Cl-LT. BP = biphenyl, CHB = cyclohexylbenzene, THDBT = tetrahydro-dibenzothiophene, and HHDBT = hexahydro-dibenzothiophene. Catalysts codes as presented in Table 1. Reaction conditions: T = 583 K, P = 5 MPa, liquid feed flow 30 mL/h, H_2/liquid feed ratio = 500 NL/L.

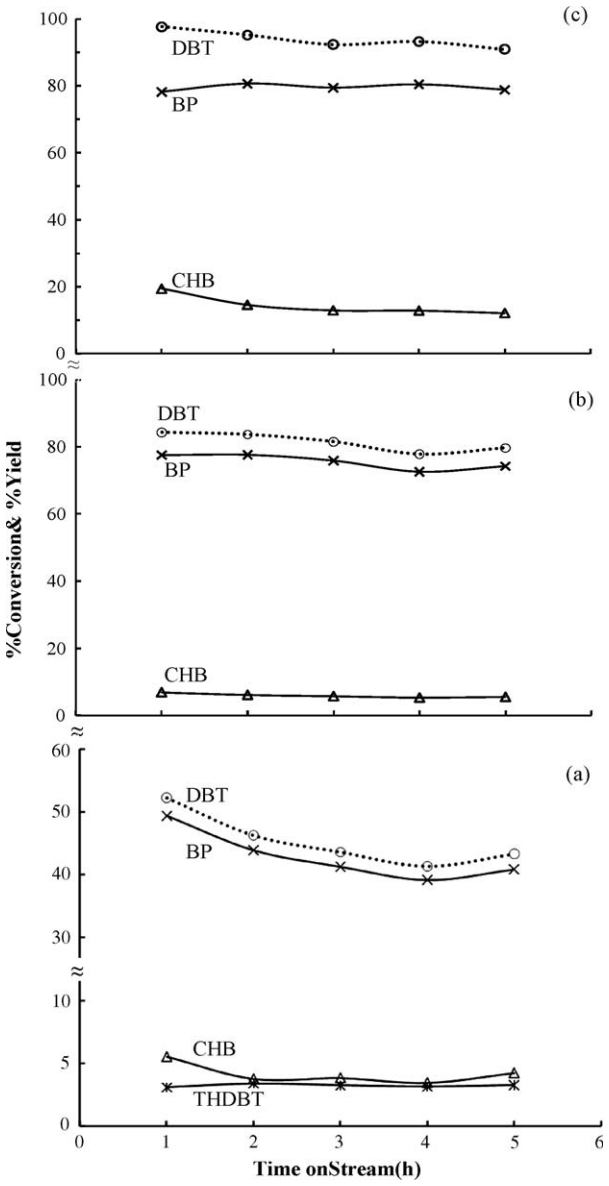

Fig. 8. Evolution with time on stream of the conversion of dibenzothiophene over the prepared Pt/γ-Al_2O_3 catalysts: (a) Pt(1.4)-Org; (b) Pt(1.1)-Cl-HT; (c) Pt(1.1)-Cl-LT.

Pt. A decrease in DBT conversion was observed for both Pt and Pd/γ-Al_2O_3 during the first 2 h of reaction, after which the steady state was attained. This can be attributed to the irreversible adsorption of sulfur on the noble metal particles [1,13]. The Pt catalysts were more active than the Pd ones, as in agreement with previous studies [3–5,11–13]. The conversion of DBT over the noble metals was a function of the nature of the metal and the preparation method. Examining the behavior of those catalysts prepared from the acetylacetonate precursors (Figs. 7a and 8a), it is noticed that, regardless of the noble metal, these catalysts were very selective to DDS, thus yielding BP as the main reaction product, and very low amounts of CHB and THDBT. Part of the DDS active sites of these two catalysts was irreversibly poisoned at the beginning of the reaction. Furthermore, it can be said that a higher number of DDS active sites of the catalysts prepared from acetylacetonates were deactivated at the beginning of the reaction as compared to those prepared from chlorides. For the catalysts prepared from chlorides, the low temperature treatment enhanced the conversion of DBT for both Pd and Pt as compared with the high temperature treatment. On the other hand, the selectivity HYD to DDS depends essentially on the nature of the noble metal for chlorided Pd and Pt/γ-Al_2O_3. Over chlorided Pd/γ-Al_2O_3 HYD becomes more competitive to DDS (Fig. 7b) and overcomes DDS when the low temperature treatment was used (Fig. 7c). In fact, it is observed that for Pd(1.4)-Cl-LT the yield to CHB is higher than the yield to BP. On the other hand, both samples of chlorided Pt/γ-Al_2O_3 were markedly selective to DDS (Fig. 8b and c). At this point, it was decided to correlate the reactivity of DBT over the different Pt and Pd/γ-Al_2O_3 catalysts and the chemical properties of these materials, in order to gain better insight into the factors that control the development of HYD over both noble metals.

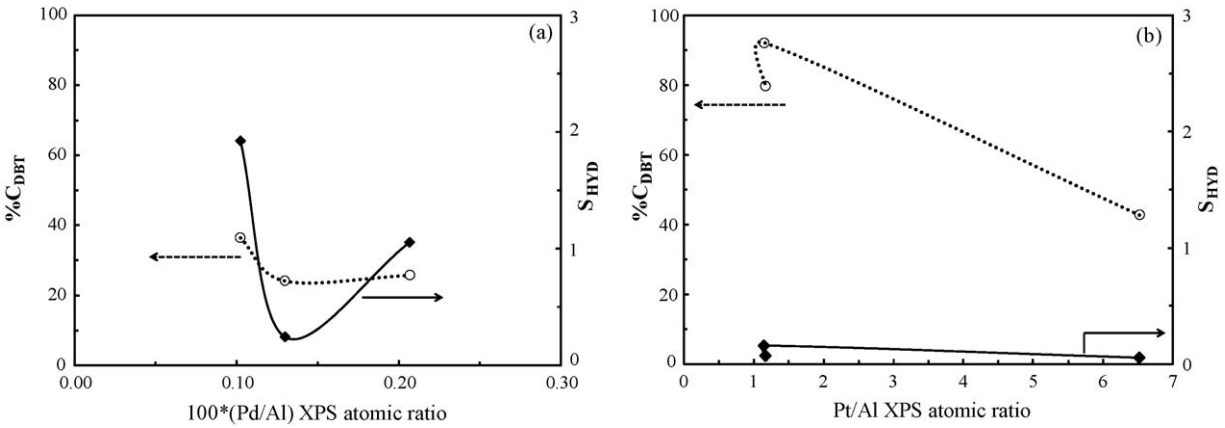

Fig. 9. Steady state conversion of DBT ($\%C_{DBT}$) and selectivity to HYD (S_{HYD}) plotted against the Pt,Pd/Al XPS atomic ratio. (a) Pd/Al and (b) Pt/Al.

3.2.1. Relationship between the dispersion of Pt and Pd and the HDS of dibenzothiophene

Fig. 9a and b features the steady state $\%C_{DBT}$ and S_{HYD} as function of the Pd/Al XPS atomic ratio (oxidized) and Pt/Al XPS atomic ratio (activated); such ratios are considered to be semi-quantitative descriptors of dispersion in supported catalysts [52–54]. It can be seen that there is no apparent correlation between these variables, regardless the noble metal. The same qualitative result can be obtained by plotting $\%C_{DBT}$ and S_{HYD} as a function of the H_2 uptake (not shown) for both noble metals. In agreement with the present results, Niquille-Röthlisberger and Prins [3] discarded particle size effects in the HDS of dibenzothiophene and 4,6-dimethylDBT over Pd and Pt/γ-Al_2O_3. Consequently, it seems reasonable to assume that the drastic changes in the catalytic performance of the prepared noble metal catalysts is rather related to the nature of the precursors, and for those materials prepared from chlorides with the change in the pretreatment conditions than to dispersion.

3.2.2. Role of the use of chloride precursors in the HDS performance of Pt and Pd/γ-Al_2O_3

As appointed before, the Pt and Pd catalysts prepared from chlorides are more active in the HDS reaction than those prepared from acetylacetonates. The presence of residual chlorine on the surface of the catalysts after activation was verified by XPS. NH_3 chemisorption measurements (Table 1) demonstrated an increase in the number of acidic sites of the chlorided catalysts. It is often considered that an increase in support's acidity enhances HDS and hydrogenation reaction rates, as well as the sulfur tolerance of noble metals [4,6,7,17–21]. This has been ascribed to the generation of electron deficient noble metal particles [17,20,21] and to the formation of additional hydrogenation sites on the metal–support interface which result from hydrogen spillover from the metal to the support [18–20,36]. The electron deficiency of Pt and Pd reduces its affinity to sulfur and therefore weakens the metal–S bonds formed during the HDS reactions [1,17,20]. On the other hand, a bifunctional HDS mechanism has been often proposed [19,55,56]. Simon et al. [19] TPD studies on the decomposition of thiophene over Pt-supported zeolites reached the conclusion that the Brønsted acidic sites of the carriers in the proximity of Pt can act simultaneously as adsorption and hydrodesulfurization sites, the HDS activity of such metal–support interface sites being significantly enhanced by spilt-over hydrogen from Pt. From NH_3 chemisorption it is not possible to distinguish between Brønsted and Lewis acidic sites, but as discussed before the use of chlorided precursors, besides an increase in the concentration of acidic sites of the catalysts, causes a change in the distribution of the weak, medium and strong acidic sites which also depends on the type of noble metal. For Pt, such redistribution mostly increases the catalytic activity but not the HYD selectivity (Fig. 8). This is not the case of Pd, for which the increase in HDS is due mainly to an enhancement of the conversion of dibenzothiophene via HYD (Fig. 7). The increase in the selectivity to HYD is particularly higher after the low temperature treatment (approximately twofold). Chou and Vannice [36] tested a series of Pd catalysts supported on several carriers of different acidic properties: C, SiO_2, Al_2O_3 SiO_2–Al_2O_3 and TiO_2, and modified the reduction temperature of those catalysts prepared from $PdCl_2$, in the hydrogenation of benzene. The highest turnover frequencies in the reaction where registered for those Pd catalysts prepared with $PdCl_2$ and reduced at low temperature (448 K). They attributed this trend to the creation of additional Brønsted acidic sites on the carrier by the action of the HCl generated during the low temperature treatment; such acidic sites being transformed into strong Lewis acidic sites with the increase in reaction temperature [36,51]. In conclusion, not only the presence of surface chlorine on the noble metals enhances the rate of HDS but the conditions of the pretreatment are very significant, in particular the reduction temperature during activation which can, aside from increasing DBT conversion, help developing the HYD route of hydrodesulfurization especially over Pd catalysts.

3.2.3. Factors controlling the development of HYD

The development of HYD is highly desirable for deep HDS. The characterization and catalytic results presented so far evidence that HYD selectivity is always low for Pt catalysts, whereas it can be modulated over Pd catalysts basically by changing the acidic balance of the Al_2O_3 carrier. It is worth the while then to consider the mechanism of hydrodesulfurization of dibenzothiophene type molecules and compare it with copious experimental evidence in the field of aromatics hydrogenation over noble metal supported catalysts, with the aim of reconciling the catalytic behavior of the present materials. To do this, it must first be reminded that the formation of a π-complex between the aromatic backbone of DBT and the catalytic active phase is a pre-requisite to HYD as in the case of aromatics hydrogenation [9,57,58] and that it has been assumed that the final sulfur withdrawal step in HYD is common to the one in DDS [3,9]. A key factor controlling all hydrogenation reactions is the intrinsic capacity of the metal to transfer hydrogen to the reacting molecule. This property is indirectly reflected by the measurements of H_2 chemisorption. It has been shown in Table 1, that the Pt catalysts have a higher H_2 uptake capacity than Pd. Such difference has been used to explain the higher intrinsic rate of hydrogenation of Pt compared to that of Pd and also linked to the development of HYD

[41] by a correlation with stereoselectivity differences in the hydrogenation of certain molecules such as o-xylene [59] and tetralin [60]. In the present work an additional factor has been encountered to play a significant role in the development of HYD over Pd; the acidic balance of the alumina carrier. It is known that alumina carriers possess mostly Lewis acidic sites [49,50] and that sulfur from H_2S [61] and thiophene [56] can be adsorbed and even dissociated over it, under certain reaction conditions [56]. Table 1 and Fig. 6 demonstrate that the γ-Al_2O_3 support and those catalysts prepared from acetylacetonates have similar acidic properties. Contrary to the chlorided catalysts, in this case both the Pt(1.4)-Org and Pd(1.8)-Org catalysts showed a high DDS selectivity. Sarbak [56] proposed that a decrease in the number of the stronger Lewis acidic sites of γ-Al_2O_3 enhances the DDS rate of hydrodesulfurization of thiophene by promoting the σ-adsorption of the molecule through the sulfur heteroatom on the weaker Lewis CUS vacancies of γ-Al_2O_3. Considering the mechanism of adsorption of the $Pt(acac)_2$ and $Pd(acac)_2$ precursors on the stronger Al^{3+} CUS sites of alumina [30] it is possible to speculate that DDS is thus favored particularly for Pd because the strong selectivity to DDS of Pt remained rather unmodified at the conditions of the present study. On the other hand, if the presence of residual chlorine particularly enhances the number of stronger Lewis acidic sites of γ-Al_2O_3 and to a certain extent the apparition of Brønsted acidic sites [49–51,56], and the noble metals are attached to the –OH groups of the carrier instead than to the Al^{3+} CUS sites of alumina this type of interaction between the DBT molecule and the support would be certainly disfavored thus promoting HYD. Furthermore, stronger Lewis acidic sites have been also proposed to play a very important role in inducing an electronic interaction between the metal and the support which causes electron deficiency of the metal particles and thus enhances the rate of hydrogenation of aromatics [62]. When the low temperature pretreatment was applied the highest activity was registered for both Pt and Pd, but whereas the HYD selectivity remained basically at the same level for Pt, it was significantly enhanced for Pd; in this case CHB became the main reaction product while the yields of THDBT and HHDBT were basically constant. As previously stated, it has been determined that when low temperature reduction of chlorided Pd catalysts is performed additional Brønsted acidic sites are created in the Al_2O_3 support as compared to reduction at higher temperatures [36,51]. Several authors [18,19,36,43] have proposed that in a bifunctional mechanism of hydrogenation these additional sites provide new hydrogenation active centers when in close proximity to the metallic phase. Such new hydrogenation sites would be responsible for the highest HYD selectivity displayed by the chlorided Pd catalyst treated at low temperature. A final aspect to be considered in establishing a relationship between the mechanism of aromatics hydrogenation and the development of HYD is that an increase in acidity conducts to a decrease in the *cis*-decalin selectivity during tetralin hydrogenation over noble metals [62,63]. Discarding the isomerization of subsequent isomerization of *cis*-decalin to *trans*-decalin it is recognized that the intrinsic increase in the selectivity to *trans*-decalin produced requires the *rollover* of the reaction intermediates over the catalytic surface [59,60,64], i.e. a consecutive adsorption–desorption of the octalin intermediate. In previous works [11,41] we have proposed that within the mechanistic dynamics of the HYD route of hydrodesulfurization of DBT also a *rollover* mechanism is involved during the change in the adsorption mode of the DBT partially hydrogenated intermediates on the active sites as to perform the final scission step of the S heteroatom. In this sense, very recent literature reports have indeed identified the presence of *cis*- and *trans*-HHDBT intermediates during the HDS of dibenzothiophene [10,65], which give support to the hypothesis of the involvement of this mechanism in the HDS of such type of compounds.

4. Conclusions

The results of this work indicated that the use of chlorided precursors to prepare γ-Al_2O_3 supported Pt and Pd catalysts enhances the conversion of dibenzothiophene at typical HDS reaction conditions. The reactivity of dibenzothiophene is linked to the type of noble metal. Thus, highly active Pt is always selective to the direct route of desulfurization, while less active Pd tends to develop the hydrogenation route of desulfurization when prepared from a chlorided precursor. Low temperature pretreatment of the chlorided catalysts, implicating reduction at 473 K, was found to enhance catalytic activity in both cases, and for Pd/γ-Al_2O_3 it doubled DBT conversion via HYD, with cyclohexylbenzene as the main reaction product. It was established that these catalytic trends are related to changes induced by residual chlorine in the chemical state of the noble metals and in particular to a modification of the distribution of weak, medium and strong acidic sites of the catalysts.

Acknowledgements

This work was possible due to the financial support of COLCIENCIAS, a government institution that promotes science and technology in Colombia, in the frame of the project 1102-06-17636. V.G. Baldovino-Medrano thanks COLCIENCIAS for a Ph.D. scholarship and UIS for financial support.

References

[1] Y. Yoshimura, M. Toba, T. Matsui, M. Harada, Y. Ichihashi, K.K. Bando, H. Yasuda, H. Ishihara, Y. Morita, T. Kameoka, Appl. Catal. A: Gen. 322 (2007) 152.
[2] H. Guo, Y. Sun, R. Prins, Catal. Today 130 (2008) 249.
[3] A. Niquille-Röthlisberger, R. Prins, J. Catal. 242 (2006) 207.
[4] V.L. Barrio, P.L. Arias, J.F. Cambra, M.B. Güemez, B. Pawelec, J.L.G. Fierro, Fuel 82 (2003) 501.
[5] V.G. Baldovino-Medrano, S.A. Giraldo, A. Centeno, Fuel 87 (2008) 1917.
[6] H.R. Reinhoudt, R. Troost, A.D. van Langeveld, S.T. Sie, J.A.R. van Veen, J.A. Moulijn, Fuel Process. Technol. 61 (1999) 133.
[7] D.D. Whitehurst, T. Isoda, I. Mochida, Adv. Catal. 42 (1998) 345.
[8] S.K. Bej, S.K. Maity, U.T. Turaga, Energy Fuels 18 (2004) 1227.
[9] H. Yang, C. Fairbridge, Z. Ring, Energy Fuels 17 (2003) 387.
[10] C.-M. Wang, T.-C. Tsai, I. Wang, J. Catal. 262 (2009) 206.
[11] V.G. Baldovino-Medrano, S.A. Giraldo, A. Centeno, J. Mol. Catal. A: Chem. 301 (2009) 127.
[12] E. Dhainaut, H. Charcosset, C. Cachet, L. de Mourgues, Appl. Catal. 2 (1982) 75.
[13] E.W. Qian, K. Otani, L. Li, A. Ishihara, T. Kabe, J. Catal. 221 (2004) 294.
[14] G. Pérot, Catal. Today 86 (2003) 111.
[15] M. Breysse, G. Djega-Mariadassou, S. Pessayre, C. Geantet, M. Vrinat, G. Pérot, M. Lemaire, Catal. Today 84 (2003) 129.
[16] F. Richard, T. Boita, G. Pérot, Appl. Catal. A: Gen. 320 (2007) 69.
[17] A. Stanislaus, B.H. Cooper, Catal. Rev.: Sci. Eng. 36 (1994) 75.
[18] L.J. Simon, J.G. van Ommen, A. Jentys, J.A. Lercher, Catal. Today 73 (2002) 105.
[19] L.J. Simon, M. Rep, J.G. van Ommen, J.A. Lercher, Appl. Catal. A: Gen. 218 (2001) 161.
[20] A.Yu. Stakheev, L.M. Kustov, Appl. Catal. A: Gen. 188 (1999) 3.
[21] W.M.H. Sachtler, Catal. Today 15 (1992) 419.
[22] E.H. Van Broekhoven, V. Ponec, Prog. Surf. Sci. 19 (1985) 351.
[23] D. Łomot, W. Juszczyk, Z. Karpiński, Appl. Catal. A: Gen. 155 (1997) 99.
[24] H. Karhu, A. Kalantar, I.J. Väyrynen, T. Salmi, D.Yu. Murzin, Appl. Catal. A: Gen. 247 (2003) 283.
[25] L.M. Tosta Simplício, S. Teixeira Brandão, E. Andrade Sales, L. Lietti, F. Bozon-Verduraz, Appl. Catal. B: Environ. 63 (2006) 9.
[26] C.-P. Hwang, C.-T. Yeh, J. Mol. Catal. A: Chem. 112 (1996) 295.
[27] P. Reyes, M. Oportus, G. Pecchi, R. Fréty, B. Moraweck, Catal. Lett. 37 (1996) 193.
[28] A.R. Sethuraman, B.H. Davis, Catal. Lett. 18 (1993) 401.
[29] H. Lieske, G. Lietz, H. Spindler, J. Völter, J. Catal. 81 (1983) 8.
[30] J.A. Rob van Veen, G. Jonkers, W.H. Hesselink, J. Chem. Soc. Faraday Trans. I 85 (1989) 389.
[31] W.A. Spieker, J.R. Regalbuto, Chem. Eng. Sci. 56 (2001) 3491.
[32] R.S. Monteiro, L.C. Dieguez, M. Schmal, Catal. Today 65 (2001) 77.
[33] J.Z. Shyu, K. Otto, Appl. Surf. Sci. 32 (1988) 246.
[34] N. Mahata, V. Vishwanathan, J. Catal. 196 (2000) 262.
[35] D.C. Koningsberger, M. Vaarkamp, Phys. B: Condens. Matter 208–209 (1995) 633.
[36] P. Chou, M.A. Vannice, J. Catal. 107 (1987) 129.
[37] J. Hancsóka, S. Magyar, K. Juhász, D. Kallo, Top. Catal. 45 (2007) 207.
[38] W. Palczewska, Adv. Catal. 24 (1975) 245.

[39] F. Bertinchamps, A. Attianese, M.M. Mestdagh, E.M. Gaigneaux, Catal. Today 112 (2006) 165.
[40] Y. Wang, R.T. Yang, J. Catal. 260 (2008) 198.
[41] V.G. Baldovino-Medrano, P. Eloy, E.M. Gaigneaux, S.A. Giraldo, A. Centeno, J. Catal. (2009), doi:10.1016/j.jcat.2009.08.004.
[42] S.D. Jackson, J. Willis, G.D. Mclellan, G. Webb, M.B.T. Keegan, R.B. Moyes, S. Simpson, P.B. Wells, R. Whyman, J. Catal. 139 (1993) 191.
[43] A. Sarkany, G. Stefler, J.W. Hightower, Appl. Catal. A: Gen. 127 (1995) 77.
[44] E. Lesage-Rosenberg, G. Vlaic, H. Dexpert, P. Lagarde, E. Freund, Appl. Catal. 22 (1986) 211.
[45] Cr. Conţescu, M.I. Vass, Appl. Catal. 33 (1987) 259.
[46] Z.C. Zhang, B.C. Beard, Appl. Catal. A: Gen. 188 (1999) 229.
[47] D. Roth, P. Gélin, M. Primet, E. Tena, Appl. Catal. A: Gen. 203 (2000) 37.
[48] G. Tonetto, M.L. Ferreira, D.E. Damiani, J. Mol. Catal. A: Chem. 171 (2001) 123.
[49] R.R. Bailey, J.P. Wightman, J. Colloid Interface Sci. 70 (1979) 112.
[50] J.B. Peri, J. Phys. Chem. 70 (1966) 1482.
[51] M. Marczewski, M. Derewinski, St. Malinowski, Can. J. Chem. Eng. 61 (1983) 93.
[52] Y. Okamoto, T. Imanaka, S. Teranishi, J. Phys. Chem. 85 (1981) 3798.
[53] B.M. Reddy, B. Chowdhury, P.G. Smirniotis, Appl. Catal. A: Gen. 211 (2001) 19.
[54] N.K. Nag, Catal. Lett. 24 (1994) 37.
[55] M. Zdražil, Appl. Catal. 4 (1982) 107.
[56] Z. Sarbak, Appl. Catal. A: Gen. 159 (1997) 147.
[57] N.K. Nag, Appl. Catal. 10 (1984) 53.
[58] J.J. Rooney, G. Webb, J. Catal. 3 (1964) 488.
[59] A.K. Neyestanaki, P. Mäki-Arvela, H. Backman, H. Karhu, T. Salmi, J. Väyrynen, D.Yu. Murzin, J. Mol. Catal. A 193 (2003) 237.
[60] S. Dokjampa, T. Rirksomboon, S. Osuwan, S. Jongpatiwut, D.E. Resasco, Catal. Today 123 (2007) 218.
[61] C.R. Apesteguia, J.F. Plaza De Los Reyes, T.F. Garetto, J.M. Parera, Appl. Catal. 4 (1982) 5.
[62] M.F. Williams, B. Fonfé, C. Woltz, A. Jentys, J.A.R. van Veen, J.A. Lercher, J. Catal. 251 (2007) 497.
[63] B.-C. Kang, T.-C. Huang, Chem. Eng. J. Biochem. Eng. J. 63 (1996) 27.
[64] Y. Inoue, J.M. Herrmann, H. Schmidt, R.L. Burwell Jr., J.B. Butt, J.B. Cohen, J. Catal. 53 (1978) 401.
[65] H. Wang, R. Prins, J. Catal. 258 (2008) 153.